NeuroImage 227 (2021) 117629

Contents lists available at ScienceDirect

NeuroImage

journal homepage: www.elsevier.com/locate/neuroimage

History of conditioned reward association disrupts inhibitory control: an examination of neural correlates

Kristin N. Meyer[a,*], Juliet Y. Davidow[b], Koene R.A. Van Dijk[c], Rosario M. Santillana[d], Jenna Snyder[d], Constanza M. Vidal Bustamante[b], Marissa Hollinshead[b], Bruce R. Rosen[c], Leah H. Somerville[b], Margaret A. Sheridan[a,d]

[a] University of North Carolina at Chapel Hill, Psychology and Neuroscience Department, 235 E. Cameron Street, Chapel Hill, NC 27599, United States
[b] Harvard University, Psychology Department and Center for Brain Science, United States
[c] Massachusetts General Hospital, United States
[d] Boston Children's Hospital at Harvard Medical School, United States

ARTICLE INFO

Keywords:
Cognitive control
Inhibitory control
Reward
fMRI
Insula
vmPFC

ABSTRACT

The neural processes that support inhibitory control in the face of stimuli with a history of reward association are not yet well understood. Yet, the ability to flexibly adapt behavior to changing reward-contingency contexts is important for daily functioning and warrants further investigation. This study aimed to characterize neural and behavioral impacts of stimuli with a history of conditioned reward association on motor inhibitory control in healthy young adults by investigating group-level effects as well as individual variation in the ability to inhibit responses to stimuli with a reward history. Participants (N = 41) first completed a reward conditioning phase, during which responses to rewarded stimuli were associated with money and responses to unrewarded stimuli were not. Rewarded and unrewarded stimuli from training were carried forward as No-Go targets in a subsequent go/no-go task to test the effect of reward history on inhibitory control. Participants underwent functional brain imaging during the go/no-go portion of the task. On average, a history of reward conditioning disrupted inhibitory control. Compared to inhibition of responses to stimuli with no reward history, trials that required inhibition of responses to previously rewarded stimuli were associated with greater activity in frontal and striatal regions, including the inferior frontal gyrus, insula, striatum, and thalamus. Activity in the insula and thalamus during false alarms and in the ventromedial prefrontal cortex during correctly withheld trials predicted behavioral performance on the task. Overall, these results suggest that reward history serves to disrupt inhibitory control and provide evidence for diverging roles of the insula and ventromedial prefrontal cortex while inhibiting responses to stimuli with a reward history.

1. Introduction

Reward history has strong and lasting influences on behavior and cognition (Anderson et al., 2016; Anderson and Yantis, 2013; Krebs et al., 2010). Yet, the ability to flexibly adapt reward-associated behavior in the context of changing goals is important for healthy functioning. Inability to overcome reward-associated responses in favor of goal-directed action may be related to risk-taking behaviors, substance use, and problematic gambling (de Ruiter et al., 2009; Galvan et al., 2006; Potenza, 2008; Robbins et al., 2012). For example, if someone has a goal of staying sober, selecting the reward-associated behavior (consuming alcohol) over the goal-directed behavior (abstaining) leads to relapse. One prominent theory of substance use indicates that cues with a history of reward (e.g. a bar), which are not themselves rewards, trigger the reward-associated behavior (e.g. consuming alcohol) (Berridge, 2012; Berridge and Robinson, 2016). While many factors contribute to the successful selection of goal-directed behavior in the context of reward-associated stimuli, a critical component is engaging cognitive control to inhibit behavioral biases driven by cues associated with a reward history. However, the specific neural mechanisms that support one's ability to engage inhibitory control in the face of stimuli with a history of reward conditioning are not well understood.

One possibility is that the regions supporting inhibitory control over stimuli with a reward history overlap with regions supporting inhibitory control in neutral contexts. Without considering reward history, goal-directed behavior is supported by a large-scale cingulo-fronto-parietal network, including anterior cingulate cortex (ACC), dorsolateral prefrontal cortex (dlPFC), inferior frontal gyrus (IFG), insular cortex, and posterior parietal cortex (Braver et al., 2009; Bush and Shin, 2006;

* Corresponding author.
E-mail address: knmeyer@live.unc.edu (K.N. Meyer).

https://doi.org/10.1016/j.neuroimage.2020.117629
Received 30 June 2020; Received in revised form 30 November 2020; Accepted 4 December 2020
Available online 13 December 2020

Cole and Schneider, 2007; Deng et al., 2018; Niendam et al., 2012). And some support for the idea that this network may support goal-directed behavior in both neutral and affective contexts comes from a recent meta-analysis suggesting that these regions are recruited for control over both neutral and emotional stimuli (Xu et al., 2016). As such, we might expect similar control regions to support inhibitory control over stimuli with a reward history.

While it is anticipated that frontal regions will support inhibitory control over reward, we also consider that regions which support a history of reward conditioning may continue to influence behavior, even after there is no longer prospect of reward receipt. For example, regions that support learning of reward-associations and habits might also perpetuate this response after the removal of reward. During reward learning, dopaminergic responses in the ventral and subsequently dorsal striatum drive stimulus-response association through reward-prediction error (Bayer and Glimcher, 2005; Pessiglione et al., 2006; Schultz et al., 1997). Additionally, the vmPFC appears to track the value of specific stimuli as they elicit preferential responses (Blair et al., 2006; Daw et al., 2006; Elliott et al., 2003; Hampton et al., 2006; Sescousse et al., 2010). It is possible that activation in these regions supporting reward-driven behavior even after the removal of reward will disrupt cognitive control. Consistent with this idea, some work has demonstrated increased striatal activation and dopaminergic activity for stimuli with a history of reward but no current reward associations (Anderson et al., 2016; Anderson et al., 2014).

Another possibility is that neural activity driving behavior due to *history* of conditioned reward association differs from neural activity associated with reward receipt. For example, the insula appears to play a crucial role in maintaining reward-related salience and modulating activity in cognitive control networks in response to such salience (Menon and Uddin, 2010). One study identified that distraction by stimuli with a reward history was associated with increased insular activity and connectivity between insula and the attentional control network (Wang et al., 2015). Further, individual differences in the change in connectivity between ventral striatum and insula during learning predicted the degree to which participants were distracted by the reward-associated stimulus (Wang et al., 2015). This suggests that the insula may serve as a relay station through which learned reward conditioning later interacts with cognitive control systems.

Here we aim to isolate the neural activity associated with the specific process of inhibitory control when encountering stimuli with a reward history. To do so, we first manipulated conditioned reward associations to initially neutral stimuli (i.e. circles and triangles) using a Monetary Incentive Delay task. After the reward conditioning phase, the stimuli that were associated with reward or were unrewarded in the Monetary Incentive Delay task were carried forward as no-go stimuli in a go/no-go task during which participants underwent functional Magnetic Resonance Imaging (fMRI) scanning and no reward was conferred. As such, we could directly compare neural signatures of inhibitory control in the face of stimuli that have a history of conditioned reward association versus inhibitory control over stimuli with equated exposure but no history of reward association. Because the testing phase of the current paradigm does not confer reward for any responses, it is equipped to isolate the process of inhibiting responses to stimuli with a history of conditioned reward association.

In sum, the basic neural functioning supporting inhibitory control over previously rewarding stimuli is still not well understood. Here we characterize neural processes subserving (1) successful inhibitory control over stimuli with a reward history, (2) failures in inhibitory control over stimuli with a reward history, and (3) the relationship between behavior during reward conditioning and neural recruitment during inhibition to previously rewarded stimuli. We firstly examined both successful and unsuccessful inhibition over reward-related stimuli as separate processes by comparing neural activity for these two types of 'no-go' stimuli. Secondly, we examined how individual differences in the ability to inhibit responses to stimuli with a reward history relates to neural activity during inhibition.

We predicted that activity in frontal and striatal regions would be preferentially active on No-Go trials with previously rewarded stimuli and that activity in these regions would be linked with task performance. Specifically, because we expected that reward conditioning, in which money is associated with fast responses to the rewarded stimulus, would lead to failures in inhibitory control, we predicted that regions involved in reward-associated motor learning (e.g., ventral and dorsal striatum), in valuation of stimuli (vmPFC), and in salience (insula) would be more active when previously rewarded stimuli are present, relative to previously unrewarded stimuli, and would disrupt performance when false alarms occur. Additionally, we hypothesized that greater recruitment of frontal control regions (e.g. ACC) would be associated with successful inhibition of previously rewarded relative to previously unrewarded stimuli.

2. Methods

2.1. Participants

Participants were 42 adults ages 18-25 years old with no self-reported history of neurological disorder, head trauma, diagnosis of any psychological or learning disorder, native language other than English, or MRI contraindications. Participants were part of a larger sample as described by Davidow and colleagues (Davidow et al., 2019). The demographic composition of the sample reflected the greater Boston area with respect to ethnicity (14% Hispanic, 82% Non-Hispanic, 5% unreported) and race (28% Asian, 2% Bi-racial, 12% Black, 49% White, and 9% unreported). One participant was excluded from final analysis due to poor task performance, defined as go accuracy less than 50% or No-Go accuracy less than 25%. This threshold ensured that participants understood and engaged with the task without penalizing individuals with lower accuracy due to legitimate challenge. The final included sample consisted of 41 individuals (49% Female, 51% Male; M-age = 21.86 years, SD = 2.20 years). All participants provided written informed consent to participate in the study and all study procedures were approved by the Partners Human Research Committee institutional review board at Massachusetts General Hospital/Harvard Medical School. For clarity, some text describing task, image acquisition, and preprocessing match as described in the study of the larger sample (Davidow et al., 2019).

2.2. Task Overview

The CARIT (adapted from (Winter and Sheridan, 2014)) consists of (a) an initial reward conditioning phase implemented using a monetary incentive delay task (MID; (Knutson et al., 2000)) and (b) an inhibitory control testing phase implemented using a go/no-go paradigm with stimuli from the conditioning phase (Fig. 1). In the conditioning phase, participants press a button as quickly as possible in response to stimuli on the screen. Reward-association is conditioned to one of the initially neutral stimuli by conferring a monetary reward for responses. For the unrewarded stimulus, participants press as quickly as possible but receive no monetary reward for responses. Reward-conditioned approach tendencies for the rewarded relative to the unrewarded stimuli are confirmed by measuring differences in reaction times. For the testing phase, the stimuli that were previously rewarded and previously unrewarded in the MID served as No-Go stimuli in the go/no-go task. The Go stimuli consisted of simple shapes with and without stripes, including a hexagon, parallelogram, pentagon, plaque, octagon, and trapezoid, that were not previously used in the MID. The testing phase was administered approximately 1 hr after the first phase. Inhibitory control is measured by successfully withholding responses to No-Go stimuli. The difference in successful trials for No-Go trails with previously rewarded stimuli and No-Go trials with previously unrewarded stimuli indicates the specific effects of reward-association history on inhibitory control. All behavioral tasks were presented in E-Prime Version 2.0 (Psychology Software Tools).

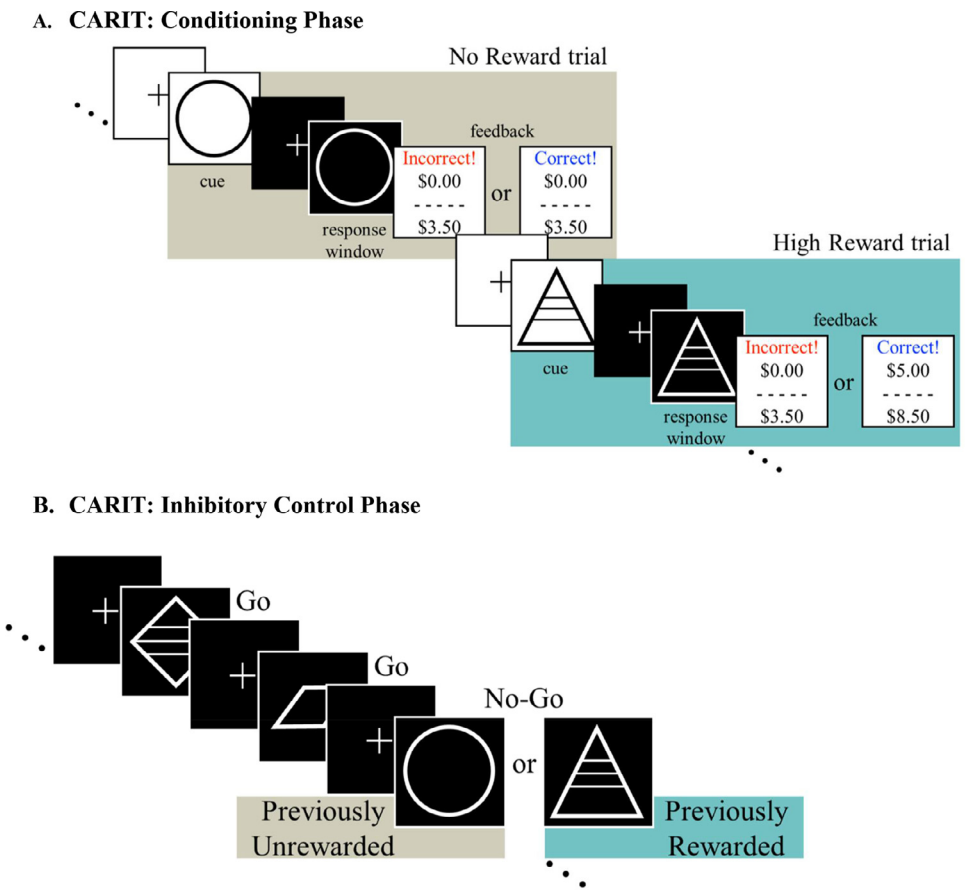

Fig. 1. CARIT. (A) Neutral cues are conditioned as targets for a buttonpress response. They are equated on number of times serving as a target but differ in reward history. One cue is reinforced with reward (high reward), and another cue is never rewarded (no reward). A feedback screen shows participants if the response was fast enough, the amount earned on the trial, and the cumulative amount earned in the block. (B) Conditioned cues become No-Go targets in the following inhibitory control task to measure the differential impact from conditioning history on inhibitory control processes. There are no rewards in the go/no-go task. Fig. modified with permission from Davidow, et al. (Davidow et al., 2019). We employed a rapid event-related design where go and No-Go target stimuli were presented for 600 ms, followed by a jittered fixation interstimulus interval ranging from 500 to 4500 ms (M = 1875 ms, SD = 1221 ms)

2.2.1. CARIT: conditioning phase

Participants completed the first study phase seated in a quiet room. Participants acquired a conditioned reward association to initially neutral stimuli (i.e., simple geometric shapes) through repeated pairing of a rapid button press and a monetary gain. Two shapes, a circle and a triangle, underwent conditioning; which shape was rewarded versus unrewarded was counterbalanced across participants. The unrewarded shape (either the circle or triangle) was never associated with a monetary outcome (no reward); all responses resulted in $0. The rewarded shape, in contrast, was associated with a monetary gain (high reward); if the participant correctly pressed during a short response window, there was a 70% chance of winning $0.50 and a 30% chance of winning $5.00, but responses that were too slow resulted in $0. Another two shapes were conditioned with a relatively small monetary gain (low reward; 70% chance of winning $0.10 and a 30% chance of winning $0.20) and risk of monetary loss (loss; 70% chance of losing $1.00 and a 30% chance of losing $5.00) but were not carried forward to the second phase of the task (the go/no-go) and are not analyzed here. There were 156 total trials with 39 trials each of the four shapes presented in an intermixed pseudorandom fashion.

In a trial (Fig. 1a), participants saw a black line drawing of a shape (500 ms) against a white background followed by a white fixation cross against a black background (jittered time interval, 2000–2375 ms, M = 2187 ms, SD = 140 ms); this change in background color signaled the participant to prepare to make a very rapid button press. Following the jittered fixation, a white line drawing of the previously cued shape appeared against the black background and participants were instructed to press a button very quickly to obtain the outcome. Immediately following, a feedback screen was presented that indicated if the response was sufficiently rapid and the resulting monetary outcome (1500 ms).

The response window adjusted dynamically during the task to control for response accuracy. Adjusting the window based on accuracy helped to equate reinforcement exposure (i.e. number of rewarded trials) across participants. A staircase algorithm adjusted the response window for each stimulus separately to set performance to approximately 66% accuracy by lengthening the response window for a stimulus if the accuracy was too low and shortening it if the accuracy was too high. The duration of the response window at the start of the task was determined by the average reaction time (RT) from a practice round immediately preceding the task.

After completing the conditioning task, we collected self-report ratings of the subjective importance, intensity, and valence of each shape on a 5-point Likert scale to verify that the repeated exposure to the different shape–outcome pairings resulted in intended changes to the subjective value of the shapes, specifically whether the high-reward shape would have greater subjective importance than the no-reward shape. The post-test assessment was not collected in one participant. Participants were paid the total amount earned in cash immediately following the self-report ratings.

2.2.2. CARIT: inhibitory control phase

The second phase of the task, which was administered during fMRI scanning, measured the degree to which the reward history acquired in the conditioning phase influenced subsequent inhibitory control behavior and associated neural processes. The high-reward and no-reward stimuli from the previous conditioning phase were carried forward to the inhibitory control phase, which we will refer to as the “previously rewarded” and “previously unrewarded” No-Go targets. Critically, in the go/no-go task, these targets no longer signal reward; there are no incen-

tives and no bonus payments for the go/no-go task. This was explicitly stated to the participants.

In the go/no-go task (Fig. 1b), participants were instructed to respond by pressing a button as rapidly as possible to a set of stimuli that appeared 73.3% of the time (go targets, 264 trials total). For the other trials, the stimulus corresponded to the previously rewarded No-Go or previously unrewarded No-Go stimuli. These were the No-Go targets, each occurring on 13.3% of trials (48 trials each; 96 total). The order of presentation for all the targets was pseudorandomized.

We employed a rapid event-related design where go and No-Go target stimuli were presented for 600 msec, followed by a jittered fixation interstimulus interval ranging from 500 to 4500 ms (M = 1875 ms, SD = 1221 ms). Correct and incorrect responses were recorded during a 1100 ms response window beginning at the onset of the target. No-Go targets were preceded by either 2, 3, or 4 'go' targets, about 1/3 of the time, a manipulation intended to impact motor prepotency. Previously rewarded No-Go and previously unrewarded No-Go targets were equally likely to be preceded by 2, 3, or 4 go targets and equally likely to be followed by all possible interstimulus intervals. Participants viewed the stimuli projected onto a screen in a mirror mounted on the head coil and used an MR-compatible button box to make behavioral responses.

2.3. Behavioral analysis

The primary outcome of interest is the comparison between the rewarded and unrewarded stimuli. For the conditioning phase, a paired t-test was conducted on reaction times to rewarded versus no-reward stimuli in order to examine whether participants responded faster to the high-reward stimulus. Additionally, subjective ratings of importance, intensity, and valence of the high-reward and no-reward stimuli were subjected to a paired t-test. For the inhibitory control phase, a similar paired t-test was conducted comparing false alarm rate to the previously rewarded No-Go and previously unrewarded No-Go stimuli.

2.4. MRI acquisition

Images were acquired at the MGH/HST Athinoula A. Martinos Center for Biomedical Imaging on a 3T CONNECTOM scanner (Fan et al., 2016; Setsompop et al., 2013) using a custom-made 64-channel phased array head coil (Keil et al., 2013). Functional BOLD images were collected in three runs of 124 volumes (total of 372 volumes) of interleaved descending T2*-weighted echo-planar (EPI) volumes at oblique transverse orientation with the following acquisition parameters: repetition time = 2500 ms, echo time = 30 ms, flip angle = 90°, array = 72 × 72, 39 slices, effective voxel resolution = 3.0 mm^3, field of view = 216 mm. A high-resolution T1-weighted multiecho magnetization-prepared rapid gradient-echo (MEMPRAGE; (van der Kouwe et al., 2008)) image, accelerated with generalized autocalibrating partially parallel acquisitions (Griswold et al., 2002) was acquired for registration purposes with the following acquisition parameters: repetition time = 2530 ms, echo time = 1.61 ms, flip angle = 7°, array = 256 × 256, 208 slices, voxel resolution = 1.0 mm^3, field of view = 256 mm.

2.5. Preprocessing

Brain imaging data processing and statistical analysis were performed in FMRIB's Software Library (FSL; (Jenkinson et al., 2012)). The MEMPRAGE image was skull-stripped using the Brain Extraction Tool (Smith, 2002), segmented into probabilistic tissue maps of gray matter, white matter, and cerebrospinal fluid using FMRIB's Automated Segmentation Tool (Zhang et al., 2001), and registration matrices were estimated for transformation into standard template space (Montreal Neurological Institute [MNI] template, voxel dimensions 2 mm^3).

Functional images were reconstructed, intensity-normalized, and then preprocessed using the fMRI Expert Analysis Tool (FEAT, v.6). Functional images were slice time-corrected using Fourier space time-series phase-shifting. Realignment estimates for correcting motion in three translational and three rotational directions were computed in MCFLIRT (Jenkinson et al., 2002), and functional images were realigned. The MEMPRAGE image was skull-stripped using the Brain Extraction Tool. Spatial smoothing was applied using a Gaussian kernel of 5 mm FWHM. Images underwent high-pass temporal filtering (Gaussian-weighted least squares straight line fitting, with sigma = 50.0 sec) and grand mean intensity normalization. The images from each scanning run were coregistered to the participant's anatomical image, and registration matrices were estimated for later linear transformation to a standard template (T1 MNI template, voxel dimensions 2 mm^3) using FLIRT (Jenkinson et al., 2002; Jenkinson and Smith, 2001).

2.6. fMRI general linear model estimation

We used a general linear model (GLM) to estimate effects of task and control for effects of non-interest. The GLM design for task events was comprised of equally weighted event onsets and durations for (1) No-Go trials where a response was successfully inhibited to the previously rewarded targets, (2) No-Go trials where a response was successfully inhibited to the previously unrewarded targets, (3) trials of failed attempts to inhibit a response to the previously rewarded targets, (4) trials of failed attempts to inhibit a response to the previously unrewarded targets, (5) trials of correctly executed responses to Go-targets, and (6) trials of missed responses to Go-targets. All task regressors were convolved with the canonical hemodynamic response function. For contrasts of the overall No-Go condition, both the regressors for previously rewarded and previously unrewarded No-Go trials were included. Following typical procedures for FSL, statistical analysis of functional images was conducted for each participant for each run, and then the runs were combined in a fixed-effect analysis for each participant, prior to submission to group mixed effects analyses. The linear registration of functional images to MNI-template space was applied in the fixed-effect analysis.

The nuisance regressors for motion consisted of 24 regressors, and were comprised of 3-translational and 3-rotational estimates of motion from realignment during preprocessing, their derivate, their square, and the square of the derivate. The 3-translational and 3-rotational estimates of motions were submitted to Art software (http://gablab.mit.edu/index.php/software) implemented through Nipype (Gorgolewski et al., 2011) to identify timepoints where there was greater than 0.9 mm relative (frame-to-frame) translations for censoring (Siegel et al., 2014) and spikes in signal intensity greater than 3 standard deviations away from the subject mean for the run. Any timepoints that exceeded this threshold were excluded. Censored timepoints were appended to the 24-column motion regressors for a set of combined nuisance regressors to append to the GLM of the task events to control for known effects of non-interest. If more than 15% of timepoints within a single run were censored this run was excluded. If a participant exhibited a single relative (frame-to-frame) movement of 5 mm or greater at any point during a run, this run was excluded. Data of one run was excluded for two participants after censoring and no participants lost more than one run of data due to excess motion.

2.7. fMRI group level statistical analysis

Group level mixed-effect statistical analyses were implemented in FEAT with FLAME1 (Eklund et al., 2016; Woolrich et al., 2004). The analysis of functional images focused on the main effects of go/no-go task event types. Because hierarchical modeling can only be used with a minimum of 3 runs, participants with fewer than 3 functional runs (i.e. participants missing any runs of data) after censoring for motion were not included in group mixed effects analyses (n = 2). Additionally, 5 participants had at least 1 run with no failed attempts to inhibit a response to the previously rewarded No-Go targets. As these participants had no

events for at least 1 run, there were fewer than 3 runs with events of interest for false alarm analyses. As such, these participants were not included in analyses of failed attempts. After these exclusions, the final sample for correctly withheld responses consisted of n = 39 participants and the final sample for false alarm trials consisted of n = 34 participants. We elected to use hierarchical modeling for analyses, because some runs included a small number of events, and hierarchical modeling includes estimates of noise around each run in the overall estimate across runs (Smith et al., 2004). Thus, although on average 34% of Previously Rewarded No-Go trials and 29% of Previously Unrewarded No-Go trials per run were false alarms, use of hierarchical modeling accounts for variation in number of events across runs and weights more heavily estimates from runs with more events.

For the general main effects of motor inhibition (No-Go collapsed across previously rewarded and previously unrewarded vs. go), fixed-effect level COPEs for each subject were modeled in a group level GLM for Go > No-Go and for No-Go > Go. To test for the influence of conditioned reward association history on inhibitory control when responses were successfully withheld, we constructed a group level GLM for correctly withheld previously rewarded No-Go > correctly withheld previously unrewarded No-Go (i.e. previously rewarded stops > previously unrewarded stops). To examine instances where reward history disrupted inhibitory control performance we examined false alarms for previously rewarded and previously unrewarded No-Go trials (previously rewarded false alarms > previously unrewarded false alarms).

To examine the relationship between task-performance and neural activity, two separate group-level GLMs were constructed where neural activity was associated with the false alarm rate to previously rewarded and previously unrewarded trials (one for previously rewarded stops > previously unrewarded stops and one for previously rewarded false alarms > previously unrewarded false alarms). All group-level results were thresholded using a voxel-wise Z-statistic threshold Z = 2.3 (p = .005) and a cluster threshold to achieve $p \leq .05$ corrected thresholding. In AFNI, cluster thresholding was determined using the AFNI 3dFWHMx program to obtain the mixed-model spatial autocorrelation function parameters from the data residuals and the AFNI 3dClustSim program to generate Monte Carlo simulations that determine the appropriate cluster size for a given voxel-wise p-value ($p < 0.005$) and overall alpha level (alpha < 0.05). Based on these simulations, clusters larger than 267-272 voxels were considered significant. All clusters reported here were larger than 272 contiguous voxels (the volume of which corresponds to 816 mm^3). Unthresholded statistical maps were uploaded to NeuroVault.org database and are available at https://neurovault.org/collections/WCSIVGXW/.

2.8. Region of interest analyses

Of primary interest was investigating how neural activity in reward-related regions and cognitive control regions relates to individual differences in behavioral task performance during both training and testing. In service of this aim, activity was extracted from 4 bilateral regions of interest (thalamus, ventral striatum, insula, and anterior cingulate cortex). The thalamus, ventral striatum, and anterior cingulate cortex were defined using coordinate values from a meta-analysis of neural activity in reward processing (Liu et al., 2011). The ROIs were created by drawing a 6-mm sphere around the voxel coordinate of the reported peak activation during anticipation of reward receipt reported in this meta-analysis. For regions in which activity was reported bilaterally in the meta-analysis (i.e. thalamus and ventral striatum), one sphere was created for the left and right hemisphere, and then these spheres were combined into a single mask so bilateral activation was extracted together. Because the insula is a larger structure, we defined this region structurally. For the insula, we used an anatomical mask using the Harvard-Oxford Probability Atlas with a 25% threshold and extracted as a singular bilateral mask. Here we used an anatomical mask because activation across both anterior and posterior insula has been evidenced in reward-driven attentional bias (Wang et al., 2015; Wittmann et al., 2010), although the meta-analysis of activation related to reward receipt only showed differences in anterior insula. Activation values were extracted from these regions using FSL's featquery.

For each ROI, regressions were conducted to investigate the association between neural activity on correct and incorrect previously rewarded No-Go trials and behavior on both the conditioning and inhibitory control phases of the CARIT. Extracted activation values for previously rewarded No-Go trials were entered into a regression as a predictor of previously rewarded No-Go false alarm rate with previously unrewarded No-Go false alarm rate and extracted previously unrewarded No-Go trial activation values entered as covariates. Similar regression analyses were conducted predicting reaction time to high-reward stimuli in the conditioning phase from previously rewarded No-Go trial activation values while controlling for previously unrewarded No-Go activation values and reaction time to no-reward stimuli. Analyses were conducted using SPSS 24. Results that survive Bonferroni correction for 4 ROIs (α = .013) are reported, including standardized beta values as estimates of effect size.

3. Results

3.1. Behavioral Results

To check the success of the conditioned reward association manipulation during the conditioning phase, differences between reaction times for high-reward trials versus no-reward trials were compared using a paired t-test. One participant had an extreme value for reward-biasing on the Monetary Incentive Delay task (i.e. difference in reaction time between rewarded and neutral stimuli), such that their reward bias was more than 3 standard deviations greater than the mean, and was thus excluded from analyses including behavior on the Monetary Incentive Delay task. Participants responded significantly faster to the high-reward stimulus than to the no-reward stimulus, $t(39) = 5.760$, $p < .001$, $d = 0.69$, see Table 1. Paired t-tests confirmed that participants rated the high-reward stimulus as more intense ($t(38) = 15.028$, $p < .001$, $d = 3.07$), more important ($t(38) = 16.962$, $p < .001$, $d = 4.00$), and of higher positive valence ($t(38) = 4.391$, $p < .001$, $d = 1.07$) than the no-reward stimulus.

The hypothesized direct effects of reward history on behavior in the inhibitory control portion of the task was examined using a paired t-test comparing false alarm rate to previously rewarded No-Go versus previously unrewarded No-Go stimuli. Results demonstrated that reward history impacted inhibitory control, as indicated by a higher false alarm rate to previously rewarded No-Go stimuli than to previously unrewarded No-Go stimuli, $t(40) = 2.347$, $p = .024$, $d = 0.32$, see Table 1. A direct relationship between biasing behavior toward reward during the conditioning phase of the CARIT and false alarms to previously rewarded stimuli in the inhibitory control phase of the CARIT was tested. Pearson correlation coefficients indicated that the difference in reaction time between high-reward and no-reward stimuli in the conditioning phase were not significantly associated with the difference in false alarm rate between the previously rewarded No-Go and previously unrewarded No-Go stimuli in the inhibitory control phase, $p = .47$.

3.2. Effect of task manipulation on neural activity- whole brain

Before examining reward-specific effects, we tested whether the expected inhibitory control regions were being recruited for No-Go trials generally. To check this, neural activation collapsing across both No-Go trial types (previously rewarded and previously unrewarded No-Go) relative to go trials was examined. Correct (stops) and incorrect (false alarms) No-Go trials were examined separately (i.e. No-Go stops > correct Go and No-Go false alarms > correct Go; see Table 2 and Fig. 2). Both of these analyses were performed because they confer differing advantages: the false alarms > correct Go contrast is equated on motoric

Table 1
Behavioral effects of reward. Mean(SD)

	Rewarded	Unrewarded	Reward Effect
MID Training (reaction time)	218 ms (20 ms)	231 ms (20 ms)	13 ms (14 ms)
Go-NoGo Testing (false alarm rate as proportion)	.32 (.16)	.28 (.140)	.05 (.13)

Table 2
Whole brain results. Negative values for X coordinates indicates left hemisphere, while positive X coordinate values correspond to right hemisphere.

			Local Maxima Coordinates				
Contrast	**Cluster**	**Size (Voxels)**	**x**	**y**	**z**	**Z-score**	**Region**
No-Go stops > correct Go	1	547	12	−68	48	4.12	Precuneus cortex
	2	1124	−30	22	−8	6.24	Inferior Frontal Gyrus
	3	1665	−32	48	14	5.00	Frontal Pole
	4	3246	−52	−46	10	4.59	Supramarginal Gyrus
	5	5195	56	−50	22	6.52	Angular Gyrus
	6	9365	30	20	6	5.79	Insular Cortex
No-Go false alarms > correct Go	1	689	4	−24	0	3.86	Right Thalamus
	2	879	22	44	26	5.63	Frontal Pole
	3	990	−60	−52	34	4.84	Supramarginal Gyrus
	4	2177	58	−48	34	5.16	Angular Gyrus
	5	2185	−30	20	−8	7.55	Insular Cortex
	6	2427	42	16	−2	7.90	Insular Cortex
	7	4750	4	26	26	6.70	Cingulate Cortex, Anterior Division
Previously rewarded stops > previously unrewarded stops	1	490	−34	14	−2	3.52	Anterior Insular Cortex
	2	636	28	28	−4	3.71	Inferior Frontal Gyrus
	3	9069	26	−94	0	5.50	Occipital Pole
			26	−10	8	3.38	Putamen
			16	−38	−4	3.18	Hippocampus
			32	−24	22	3.15	Posterior Insula
			18	10	14	3.14	Caudate
Previously rewarded false alarms > previously unrewarded false alarms	1	430	−48	−14	22	3.5	Central Opercular Cortex
	2	535	−24	−96	−4	4.22	Occipital Pole
			14	−38	−4	3.61	Hippocampus
			−6	−78	46	3.32	Superior parietal lobule
			−48	−14	22	3.41	Posterior Insula
	3	3749	0	−82	30	4.88	Cuneal Cortex
			−28	−6	12	2.38	Putamen

response (i.e. pressing) between No-Go and Go trials while the stops >correct Go differs in motoric response but is equated on accuracy. Results replicate previous go/no-go studies, in which participants engaged regions associated with inhibitory control including the right inferior frontal gyrus (rIFG).

Group maps of correctly withheld previously rewarded No-Go > correctly withheld previously unrewarded No-Go (previously rewarded stops > previously unrewarded stops) demonstrate that differences in the history of conditioned reward-association for a stimulus yielded different patterns of neural activation, even on trials when this reward history did not disrupt behavior (Table 2; Fig. 3). Relative to previously unrewarded successful stop trials, previously rewarded successful stop trials elicited greater activity bilaterally in the IFG, insula, striatum, thalamus, caudate, lateral occipital cortex, and pericalcarine cortex. We also examined neural responses to previously rewarded > previously unrewarded trials when inhibitory control failed, during false alarm trials (previously rewarded false alarms > previously unrewarded false alarms). This contrast elicited activation in the insula, lateral occipital cortex, and pericalcarine cortex (Table 2; Fig. 4). When the inverse of this comparison was tested (previously unrewarded > previously rewarded) no significant activation was observed for correct or incorrect trials.

3.3. Association between neural activity and task performance – whole brain

To further investigate how differences in activity between previously rewarded and previously unrewarded No-Go trials relate to behavior, a whole brain analysis was conducted where both previously rewarded and previously unrewarded false alarm rate were included in a group level GLM as covariates of interest. The covariates of previously rewarded false alarm rate and previously unrewarded false alarm rate were correlated, $r(39) = .62$, $p < .01$, but with a low level of multicollinearity (Variance Inflation Factor = 1.64 for previously rewarded and previously unrewarded false alarm rate in regression predicting extracted vmPFC activity) indicating that it is acceptable to include both previously rewarded and previously unrewarded false alarm rate as predictors. For the previously rewarded correct stops > previously unrewarded correct stops contrast, false alarm rate to previously rewarded stimuli relative to previously unrewarded stimuli correlated with neural activity in the vmPFC (592 voxel cluster size; local maximum x = -4, y = 58, z = 4). To better visualize this relationship, this activity was extracted and plotted against task performance (Fig. 5). Greater vmPFC activity on correctly withheld previously rewarded No-Go trials relative to previously unrewarded No-Go trials was associated with a lower false alarm rate for previously rewarded relative to previously unrewarded stimuli. For the previously rewarded false alarms > previously unrewarded false alarms contrast, false alarm rate to previously rewarded relative to previously unrewarded No-Go trials correlated with neural activity in the lateral occipital cortex (1228 voxel cluster size; local maximum x = -18, y = -80, z = 38).

3.4. Association between neural activity and task performance – regions of interest

In order to test how the frontal and striatal regions of interest related to overall ability to inhibit responses to stimuli with a reward-related history, regressions were conducted to investigate the association be-

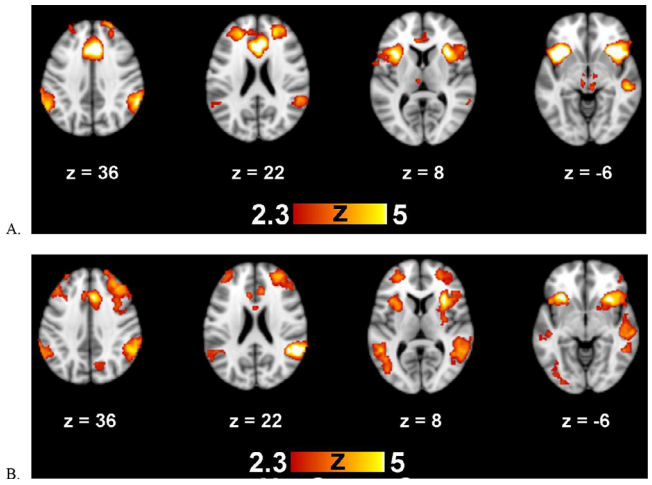

Fig. 2. *A.* False Alarm No-Go trials (collapsed across previously rewarded and previously unrewarded) > correctly pressed go trials, $p < .05$, FWE corrected clusterwise. *B.* Correctly withheld No-Go trials (collapsed across previously rewarded and previously unrewarded) > correctly pressed go trials, $p < .05$, FWE corrected clusterwise. Unthresholded statistical maps were uploaded to NeuroVault.org database and are available at https://neurovault.org/collections/WCSIVGXW/.

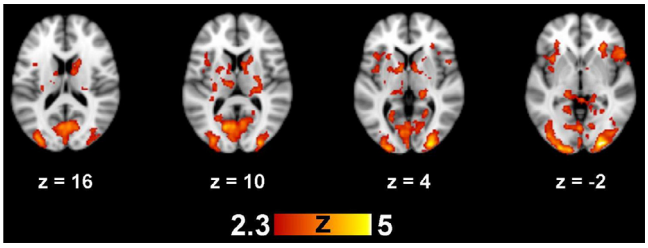

Fig. 3. Whole brain activation for correctly withheld previously rewarded trials > correctly withheld previously unrewarded trials, $p < .05$, FWE corrected. Unthresholded statistical maps were uploaded to NeuroVault.org database and are available at https://neurovault.org/collections/WCSIVGXW/.

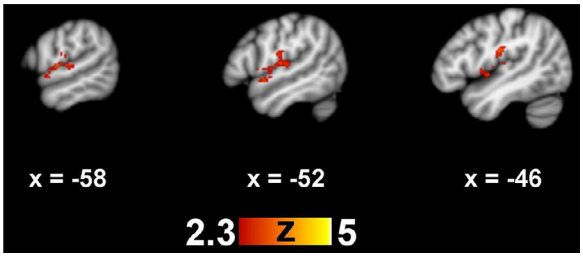

Fig. 4. Whole brain activation for false alarms to previously rewarded > false alarms to previously unrewarded, $p < .05$, FWE corrected clusterwise. Unthresholded statistical maps were uploaded to NeuroVault.org database and are available at https://neurovault.org/collections/WCSIVGXW/.

tween neural activity for each ROI on correct and incorrect previously rewarded > previously unrewarded trials and behavior. For correct trials, no activity in these ROIs significantly predicted behavior (all *p*'s > .10). For incorrect trials, more activity in the Thalamus ($\beta = .381$, $p = .012$, Fig. 6) and Insula ($\beta = .440$, $p = .004$, Fig. 6) to previously rewarded false alarm trials > previously unrewarded false alarm trials predicted more false alarms on previously rewarded No-Go trials relative to previously unrewarded No-Go trials. No other regions significantly predicted the previously rewarded > previously unrewarded false alarm rate (all *p*'s > .05).

3.5. Relationship monetary incentive delay – ROI analysis

Regression analyses were performed to analyze the relationship between prior learning performance during conditioned reward-association and neural activity during later inhibitory control over reward. Reward-biasing on the MID task (e.g. difference in reaction time between rewarded and neutral stimuli) predicted neural recruitment in the insula ($\beta = .536$, $p = .001$, Fig. 7) during previously rewarded false

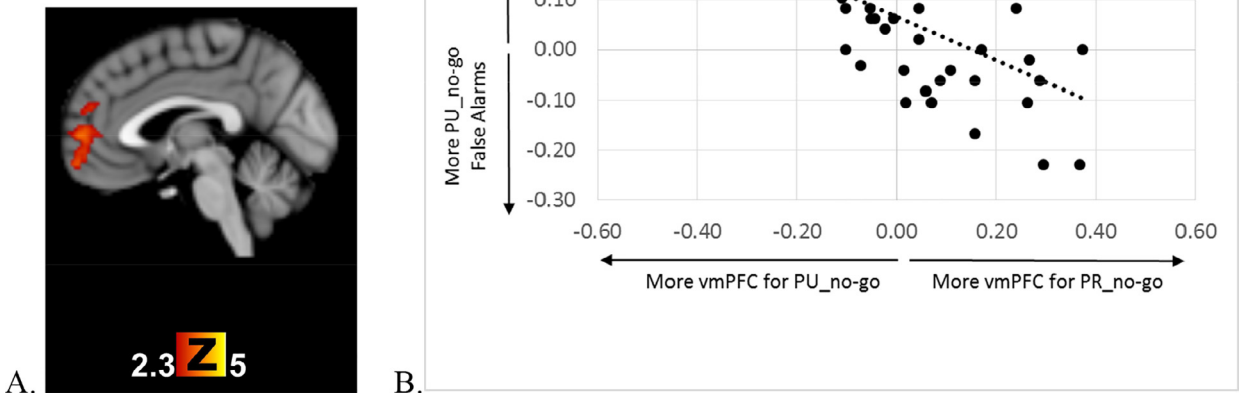

Fig. 5. *A.* Results of whole brain correlation with behavior at x = -2, $p < .05$, FWE corrected clusterwise. Results show that greater vmPFC activity to previously rewarded No-Go stimuli relative to previously unrewarded No-Go stimuli on correctly withheld trials predicted fewer false alarms to previously rewarded stimuli relative to previously unrewarded stimuli. Unthresholded statistical maps were uploaded to NeuroVault.org database and are available at https://neurovault.org/collections/WCSIVGXW/. *B.* Scatterplot of activation extracted from the vmPFC cluster displayed for descriptive purposes only.

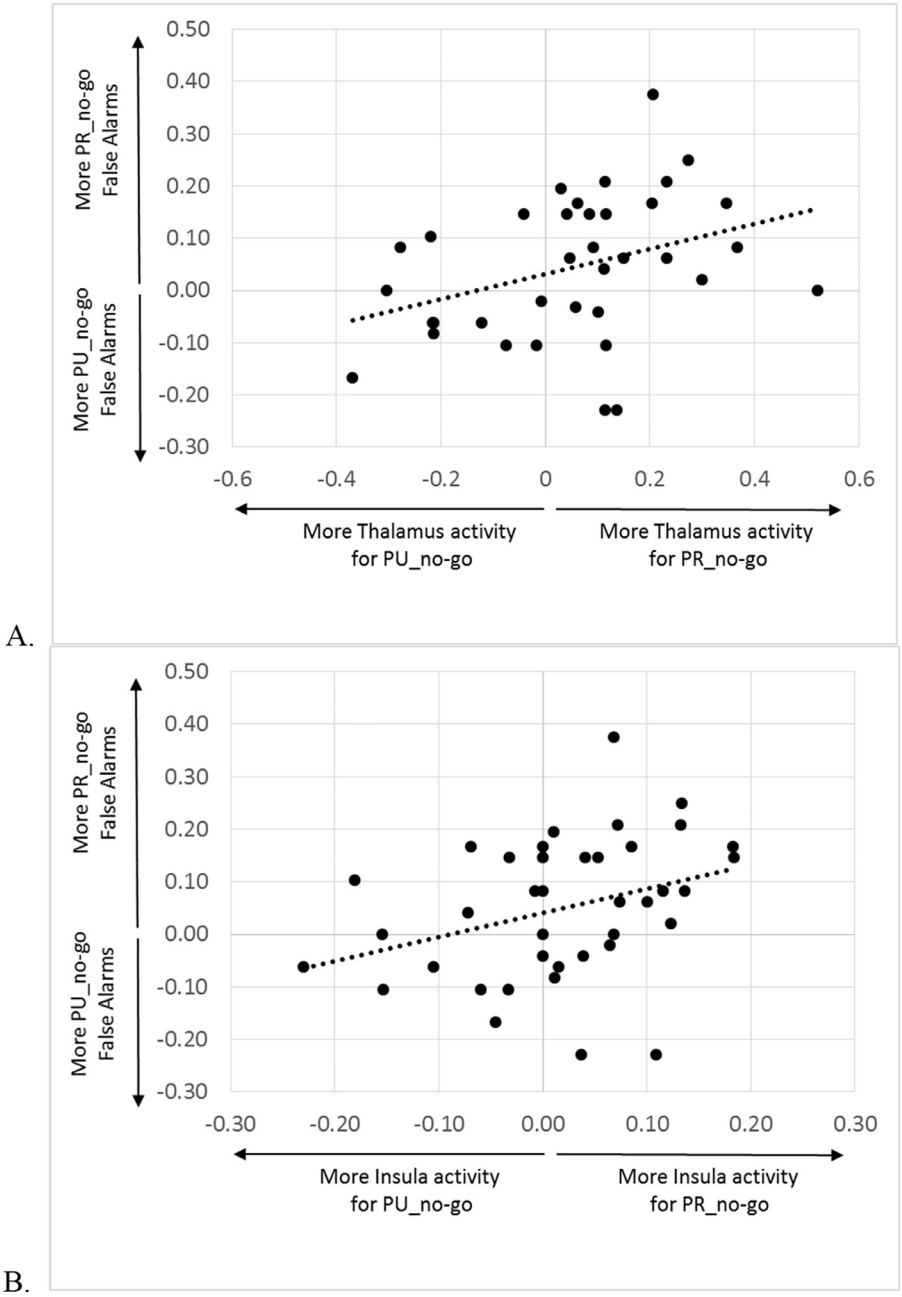

Fig. 6. *A.* Partial plot of bilateral thalamic activity on false alarm trials for the contrast previously rewarded > previously unrewarded predicting previously rewarded false alarm rate, while controlling for previously unrewarded false alarm rate. *B.* Partial plot of bilateral Insula activity on false alarm trials for the contrast previously rewarded > previously unrewarded predicting previously rewarded false alarm rate, while controlling for previously unrewarded false alarm rate.

alarm > previously unrewarded false alrm trials. Greater differences in reaction time between rewarded and unrewarded stimuli on the MID task predicted greater activity in insula when failing to inhibit responses to previously rewarded No-Go stimuli. There were no such associations for behavior on the MID task and activity on previously rewarded correct stop > previously unrewarded correct stop trials (all *p*'s > .09).

3.6. *Post-Hoc analysis: subdivisions of the insula*

Additional post-hoc analyses were performed to test whether the original analysis, which extracted activation across the whole of the structural insula, was the best representation of the data. Additional analyses were conducted because there is evidence for distinct connectivity patterns between the dorsal anterior insula, ventral anterior insula, and posterior insula that also reflect differences in function (Cauda et al., 2011; Deen et al., 2011). To conduct these analyses, ROI's were created utilizing the 400 parcel solution from a parcellation-based analysis conducted by Schaefer and colleagues (2018; https://github.com/ThomasYeoLab/CBIG/tree/master/stable_projects/brain_parcellation/Schaefer2018_LocalGlobal). Parcels were identified that most closely matched the locations of ventral anterior (Left Hemisphere: 104; Right Hemisphere: 309), dorsal anterior (Left Hemisphere: 89-91; Right Hemisphere: 291-293), and posterior (Left Hemisphere: 46-47; Right Hemisphere: 246-248) insula. From these parcels, 3 ROI masks were created which included bilateral ventral anterior insula, bilateral dorsal anterior insula, and bilateral posterior insula. Activations were extracted from these regions and subjected to the same analyses performed on the whole structural insula as reported above.

3.6.1. *Subdivisions of the insula: association between neural activity and task performance*

Regressions were conducted to investigate the association between neural activity for each ROI on incorrect Previously Rewarded No-Go

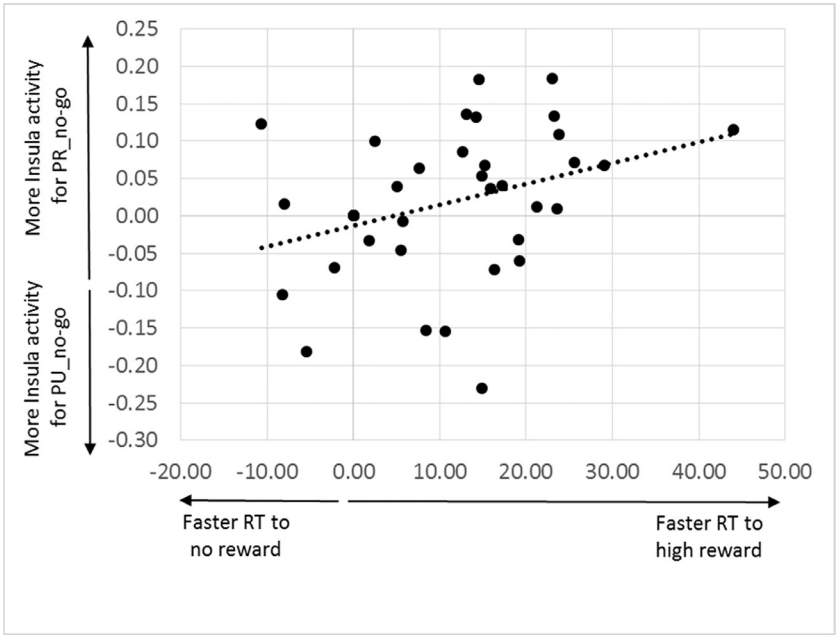

Fig. 7. Plot of reward biasing on the MID, as measured by RT difference between high reward and no reward stimuli, predicting neural activity in the insula on false alarms to previously rewarded No-Go stimuli.

> Previously Unrewarded No-Go trials and behavior. Significantly more activity in the dorsal anterior insula ($\beta = .353$, $p = .017$), the posterior insula ($\beta = .455$, $p = .002$), and trending in the ventral anterior insula ($\beta = .294$, $p = .083$) for Previously Rewarded > Previously Unrewarded false alarm trials predicted overall more false alarms on the Previously Rewarded relative toe Previously Unrewarded No-Go trials.

Subdivisions of the Insula: Relationships with Monetary Incentive Delay

Reward-biasing on the Monetary Incentive Delay task (e.g. difference in reaction time between rewarded and neutral stimuli) predicted neural recruitment in the dorsal anterior insula ($\beta = .370$, $p = .024$) and in the ventral anterior insula ($\beta = .303$, $p = .035$) during Previously Rewarded > Previously Unrewarded false alarm trials, such that greater differences in reaction time between rewarded and unrewarded stimuli on the Monetary Incentive Delay task predicted greater activity in ventral anterior and dorsal anterior insula when failing to inhibit responses to Previously Rewarded Stimuli. Results for this analysis using posterior insula activation values was in the same direction but did not reach significance ($\beta = .238$, $p = .139$).

4. Discussion

This study aimed to characterize neural and behavioral impacts of a history of reward conditioning on motor inhibitory control in healthy young adults by investigating group-level effects as well as individual variation in the ability to inhibit to previously rewarding stimuli. Participants first underwent conditioned reward association training, and then the rewarded and unrewarded stimuli from the conditioning phase served as No-Go targets in a go/no-go task to test the effect of reward history on inhibitory control. On average, a history of reward conditioning disrupted inhibitory control. Trials with previously rewarded No-Go stimuli were linked with greater activity in frontal and subcortical regions, including IFG, insula, striatum, and thalamus, relative to trials with previously unrewarded No-Go stimuli. For both the previously rewarded and previously unrewarded No-Go stimuli, participants had successful (correctly inhibited) and unsuccessful (false alarm) attempts. Previous work has more often focused on neural correlates for successful trials (Anderson, 2017; Anderson et al., 2014; Davidow et al., 2019), however this study provided opportunity to dissociate neural signatures related to successful control over previous reward versus failures in control over reward. By analyzing these trial types separately, we were able to both examine which regions support inhibitory control over reward and disrupt inhibitory control over reward.

Greater activity in the insula and thalamus on false alarms was associated with overall greater disruption in inhibitory control over reward related stimuli. In contrast, greater activity in the vmPFC on correctly withheld trials predicted better inhibitory control over reward. Activity in the insula during the inhibitory control phase (but no other regions) was linked both with behavior during reward conditioning and behavior on the go/no-go task. Of the regions examined, the insula was the only region for which activity was linked with behavior both during the reward conditioning phase and during the unrewarded inhibitory control phase. Our results suggest that history of reward conditioning serves to disrupt inhibitory control. Additionally, given the insula's relationship to both reward conditioning and inhibitory disruption, the insula may serve as an important intermediary relay-station through which history of reward interacts with current control demands and warrants further investigation.

4.1. Failures in inhibitory control over reward-associated stimuli

The experiment was separated into an initial conditioned reward association phase and a second inhibitory control phase. During the reward conditioning phase, participants pressed a button in response to initially neutral stimuli. Button press to one of the stimuli was associated with monetary reward whereas pressing to another stimulus was not associated with any reward. Thus, these stimuli did not differ in number of times serving as a target but did differ in their reward history. Consistent with behavior being biased by reward, participants responded more quickly to the rewarded than the unrewarded stimulus. Further, when these same stimuli were carried forward in a go/no-go task, participants were overall worse at inhibiting responses to the stimulus that had been previously associated with reward in the conditioning phase than the stimulus that was previously unrewarded in the conditioning phase. This approach also allowed us to extend previous findings from reversal-learning paradigms. Whereas for reversal learning paradigms, a previously rewarded response-outcome association is replaced with a novel response-outcome association, here we specifically isolated disruption in suppression of a previously rewarded response without also confounding learning a novel response-outcome association.

We sought to identify which neural regions might play a role in this carry-over effect of history of reward-association leading to disruptions

in inhibitory control. We demonstrate that the degree to which participants increased the speed of their responses to rewarded stimuli in the conditioning phase was linked with the degree to which the insula was active when participants made a false alarm response to previously rewarded stimuli in the inhibitory control phase. More insula activity while making false alarms to previously rewarded stimuli was also related to the false alarm rate to previously rewarded stimuli.

Previous work has demonstrated that the insula is important for responding to salient events and stimuli (Seeley et al., 2007; Uddin, 2015) and is involved in reward processing (Knutson et al., 2000; Lee and Shomstein, 2013; Pessoa and Engelmann, 2010). One study extended this work to examine insular activity in an attentional control task after acquisition of reward-association, demonstrating that initial reward learning interfaces with later attentional control through the insula, supporting the role of the insula as an intermediary relay station through which reward history affects cognitive control (Wang et al., 2015). Finally, theoretical frameworks posit that the insula modulates control over actions, particularly in less predictable environments, based upon motivationally salient stimuli in the environment (Tops and Boksem, 2011). Taken together, theory and empirical evidence suggests that the insula may serve as a candidate region as an intermediary through which motivational reward history subsequently biases cognitive control even after the prospect of reward is no longer available. One complementary role the insula may be playing is that of saliency detection of the previously rewarded stimulus. Previous evidence highlights the role of the insula in saliency detection, such as during error processing and sensory-driven salience (Cai et al., 2017). Future work should further clarify the specific role of the insula in supporting interactions between reward conditioning and cognitive control.

We also examined the possibility that some subdivisions of the insula may play differing roles in this intermediary process. Specifically, functional parcellation of the insula suggests there are subdivisions of the insula, with most analysis indicating three subregions of the insula (Chang et al., 2013; Deen et al., 2011). These include the posterior insula, which supports sensorimotor and interoceptive processing (Craig, 2002; Wager et al., 2004), the ventral anterior insula, which appears engaged during affective tasks, and the dorsal anterior insula, which appears relatively more engaged during executive functioning tasks (Kurth et al., 2010), our pattern of results is largely similar across these subregions of the insula. This may be in part because the task in which we are examining insula activity engages elements of each of these processes, including motor control, executive functioning, and reward-associated salience.

In addition to the insula, we found that greater activity in the thalamus for previously rewarded relative to previously unrewarded stimuli during false alarms was related to worse inhibitory control over previously rewarded stimuli. The thalamus receives input from the striatum via direct and indirect pathways and projects to the motor cortex, and in turn serves to integrate reward-related motivation and action selection (Bosch-Bouju et al., 2013; Corbit et al., 2003; Lanciego et al., 2012; Wickens et al., 2003). Previous work has linked thalamic activity with invigorated motor responses and reward response (Gaidica et al., 2018; Liu et al., 2011; Rademacher et al., 2010), both of which are consistent with our findings demonstrating links between thalamic activity and false alarm rate to previously rewarded stimuli.

4.2. Successful inhibitory control over reward-associated stimuli

While participants, on average, demonstrated more failures in inhibitory control to previously rewarded than previously unrewarded stimuli, there was variability in this effect both across trials and across participants. In an effort to test which regions support better inhibitory control over reward, we examined how neural activity on successful trials related to overall ability to withhold responses to previously rewarded stimuli. A whole brain investigation of relationships between neural activity on correct trials and behavioral performance revealed that greater vmPFC activity to previously rewarded relative to previously unrewarded stimuli on correct trials predicted better ability to withhold responses to previously rewarded relative to previously unrewarded stimuli. The vmPFC supports behavioral flexibility in the context of changing reward contingencies (Bechara et al., 2000; Fellows and Farah, 2003), and this region is involved in updating relationships between potential actions and reward outcomes (Gläscher et al., 2009). In the current study, participants initially learn an association between pressing to the rewarded stimulus and a reward outcome in the conditioning phase, and subsequently are required to update this relationship as the prospect of reward is removed and a different response (withholding) is aligned with task goals. The sample from which this study was taken, which also included children and adolescents, found that IFG and vmPFC coactivation while inhibiting to the previously rewarded stimulus increased with age, which paralleled an increasing behavioral effect of reward history with age (Davidow et al., 2019). Additionally, the adults who showed the highest vmPFC-IFG coactivation also showed the greatest recovery across time, which may indicate a role for the vmPFC in updating outcomes (Davidow et al., 2019). Similarly, our results show that greater vmPFC activity is associated with better ability to inhibit responses to previously rewarded stimuli, which may reflect reversing an action-outcome association and is consistent with studies of reversal learning which identify this role for the vmPFC (Fellows and Farah, 2003; Zhang et al., 2016).

We also hypothesized that while successfully inhibiting a response to a previously rewarded stimuli, frontal control areas would be recruited. On average there was greater activity in the IFG for successful inhibition to previously rewarded relative to previously unrewarded stimuli. We additionally expected that differences in ACC activity would be observed and would relate to task performance. While previous work demonstrates that ACC supports conflict resolution and monitoring during inhibition (Botvinick et al., 2004; Verbruggen and Logan, 2008), our results suggest that ACC activity does not differ when supporting inhibition over stimuli with or without a history of conditioned reward-association. The IFG supports successful inhibition to neutral stimuli in inhibitory control tasks (Aron et al., 2014; Swick et al., 2008), and shows increases in activity corresponding to increases in difficulty in inhibition (Hughes et al., 2013). Given that participants show more difficulty inhibiting to previously rewarded stimuli, the increase in IFG activity for previously rewarded stimuli may be supporting the resolution of increased demands of inhibition when at odds with an action previously associated with reward.

4.3. Limitations and future directions

While this study provided novel insight into how reward history disrupts inhibitory control in typically functioning adults, there are limitations to consider and future avenues for research. Firstly, because we measured neural function during the go/no-go task, but not during initial conditioned reward-association on the Monetary Incentive Delay task, future work is required to investigate which regions recruited during reward learning impact later disruption in inhibitory control. Secondly, while this project examined how a specific facet of cognitive control (inhibition) interacts with reward history, more work is needed to clarify how these findings generalize to cognitive control and reward interactions more broadly. Our findings in the inhibitory control domain replicate and extend previous findings in the attention domain (Wang et al., 2015), suggesting that the insula may serve as a relay station through which reward history and cognitive control interact. As such, it is likely that the insula serves this function across cognitive control domains, and this warrants further investigation. Thirdly, it is as of yet unclear why we do not find a relationship between behavior during the reward conditioning phase and inhibitory control phase in this study. It may be due to noise around behavioral estimates of behavior during learning, particularly given that difficulty is dynamically ad-

justed based upon performance. Future studies may benefit from testing whether there is evidence for a relationship with more proximal measures of reward response, such as a relationship between striatal activity during learning and later inhibitory control. Finally, this work further highlights the interplay between reward history and inhibitory control, which warrants further examination. Our results demonstrate that reward history disrupts inhibitory control and that successful inhibition over previously rewarded stimuli may be supported by vmPFC activity. Related work has found that inhibiting responses to previously rewarded stimuli leads to devaluation of those stimuli (Wessel et al., 2014; Wessel et al., 2015). This suggests that the relationship between value and inhibition may be bidirectional in nature, wherein value history leads to worse inhibitory control and inhibition itself leads to devaluation. Future work should capitalize on these findings to investigate ways in which inhibition over previously rewarded stimuli can be supported in service of both devaluation and successful inhibition, such as through inhibitory control training.

In conclusion, this study characterized neural substrates associated with successful and unsuccessful inhibition to previously rewarded stimuli, relative to stimuli with no history of reward, in typically functioning young adults. We provide evidence that a history of reward-association with a button-press response for one stimulus leads to worse inhibitory control over that stimulus in a subsequent task. Behavior biased toward reward during learning and behavior disrupted by reward history during the unrewarded inhibitory control phase are associated with greater activity in the insula during false alarm trials, which provides support for the insula being an interface between reward learning and subsequent effects on cognitive control. While greater insula activity was linked with worse performance, greater vmPFC activity during successful inhibition over reward is associated with better performance for previously rewarded relative to unrewarded stimuli. Taken together, this suggests that the vmPFC may contribute to successful motor inhibition in the face of previous reward whereas insula may bias behavior toward previously rewarded actions and stimuli, even when such behavior is at-odds with current goals.

Declaration of Competing Interest

None.

Credit authorship contribution statement

Kristin N. Meyer: Formal analysis; conceptualization; data curation; writing - original draft; writing- review and editing. **Juliet Y. Davidow:** Conceptualization; formal analysis; data curation; writing review & editing. **Koene R.A. Van Dijk:** Investigation. **Rosario M. Santillana:** Investigation; data curation. **Jenna Snyder:** Investigation; data curation; project administration. **Constanza M. Vidal:** Investigation: data curation. **Marissa Hollinshead:** Investigation. **Bruce R. Rosen:** Funding acquisition; supervision. **Leah H. Somerville:** Supervision; funding acquisition; methodology; conceptualization; writingreview & editing. **Margaret A. Sheridan:** Supervision; funding acquisition; methodology; conceptualization; writing-review editing; writing- original draft.

Data availability

Unthresholded activation maps for this study have been made available as a collection on NeuroVault (https://neurovault.org/collections/WCSIVGXW/).

Acknowledgments

The authors thank Randy Buckner and Thomas Witzel for helpful comments and support throughout the study; Boris Keil for technical support; Elizabeth Beam, Michelle Drews, Aya Hamadeh, and Emily Shaw for help with data collection; and Megan Garrad for help with participant recruitment. This project was supported by a National Institutes of Health Blueprint Initiative for Neuroscience Research Grant (U01 MH93765) to B.R.R., a Harvard University Mind, Brain, and Behavior Interfaculty Initiative Grant to M.A.S. and L.H.S., a National Institute for Drug Abuse Grant (R03 DA037405) to M.A.S, and a National Science Foundation Graduate Research Fellowship (DGE-1650116) to K.N.M. Funding sources were not involved in study design, collection, analysis, interpretation, writing, or decision to submit the article for publication.

Supplementary materials

Supplementary material associated with this article can be found, in the online version, at doi:10.1016/j.neuroimage.2020.117629.

References

Anderson, B.A., 2017. Reward processing in the value-driven attention network: reward signals tracking cue identity and location. Soc. Cognit. Affect. Neurosci. 12 (3), 461–467. doi:10.1093/scan/nsw141.

Anderson, B.A., Folk, C.L., Garrison, R., Rogers, L., 2016. Mechanisms of habitual approach. J. Experiment. Psychol. General 145 (6), 796–805. doi:10.1037/xge0000169.

Anderson, B.A., Kuwabara, H., Wong, D.F., Gean, E.G., Rahmim, A., Brašić, J.R., …, Yantis, S., 2016. The role of dopamine in value-based attentional orienting. Curr. Biol. 26 (4), 550–555. doi:10.1016/j.cub.2015.12.062.

Anderson, B.A., Laurent, P.A., Yantis, S., 2014. Value-driven attentional priority signals in human basal ganglia and visual cortex. Brain Res. 1587, 88–96. doi:10.1016/j.brainres.2014.08.062.

Anderson, B.A., Yantis, S., 2013. Persistence of value-driven attentional capture. J. Exp. Psychol. Hum. Percept. Perform. 39 (1), 6–9. doi:10.1037/a0030860.

Aron, A.R., Robbins, T.W., Poldrack, R.A., 2014. Inhibition and the right inferior frontal cortex: one decade on. Trends Cogn. Sci. 18 (4), 177–185. doi:10.1016/j.tics.2013.12.003.

Bayer, H.M., Glimcher, P.W., 2005. Midbrain dopamine neurons encode a quantitative reward prediction error signal. Neuron 47 (1), 129–141. doi:10.1016/j.neuron.2005.05.020.

Bechara, A., Tranel, D., Damasio, H., 2000. Characterization of the decision-making deficit of patients with ventromedial prefrontal cortex lesions. Brain 123 (11), 2189–2202. doi:10.1093/brain/123.11.2189.

Berridge, K.C., 2012. From prediction error to incentive salience: mesolimbic computation of reward motivation. Eur. J. Neurosci. 35 (7), 1124–1143. doi:10.1111/j.1460-9568.2012.07990.x.

Berridge, K.C., Robinson, T.E., 2016. Liking, wanting, and the incentive-sensitization theory of addiction. Am. Psychol. 71 (8), 670–679. doi:10.1037/amp0000059.

Blair, K., Marsh, A.A., Morton, J., Vythilingam, M., Jones, M., Mondillo, K., …, Blair, J.R., 2006. Choosing the lesser of two evils, the better of two goods: specifying the roles of ventromedial prefrontal cortex and dorsal anterior cingulate in object choice. J. Neurosci. 26 (44), 11379–11386. doi:10.1523/JNEUROSCI.1640-06.2006.

Bosch-Bouju, C., Hyland, B.I., Parr-Brownlie, L.C., 2013. Motor thalamus integration of cortical, cerebellar and basal ganglia information: implications for normal and parkinsonian conditions. Front. Computat. Neurosci. 7. doi:10.3389/fncom.2013.00163.

Botvinick, M.M., Cohen, J.D., Carter, C.S., 2004. Conflict monitoring and anterior cingulate cortex: an update. Trends Cogn. Sci. 8 (12), 539–546. doi:10.1016/j.tics.2004.10.003.

Braver, T.S., Paxton, J.L., Locke, H.S., Barch, D.M., 2009. Flexible neural mechanisms of cognitive control within human prefrontal cortex. PNAS 106 (18), 7351–7356. doi:10.1073/pnas.0808187106.

Bush, G., Shin, L.M., 2006. The Multi-Source Interference Task: an fMRI task that reliably activates the cingulo-frontal-parietal cognitive/attention network. Nature Protocols; London 1 (1), 308–313. doi:10.1038/nprot.2006.48, http://dx.doi.org/.

Cai, W., Chen, T., Ide, J.S., Li, C.-S.R., Menon, V., 2017. Dissociable fronto-operculum-insula control signals for anticipation and detection of inhibitory sensory cue. Cereb. Cortex 27 (8), 4073–4082. doi:10.1093/cercor/bhw219.

Cauda, F., D'Agata, F., Sacco, K., Duca, S., Geminiani, G., Vercelli, A, 2011. Functional connectivity of the insula in the resting brain. Neuroimage 55 (1), 8–23. doi:10.1016/j.neuroimage.2010.11.049.

Chang, L.J., Yarkoni, T., Khaw, M.W., Sanfey, A.G., 2013. In: Decoding the Role of the Insula in Human Cognition: Functional Parcellation and Large-Scale Reverse Inference, 23. Cerebral Cortex, New York, N.Y., pp. 739–749. doi:10.1093/cercor/bhs065 1991https://doi.org/.

Cole, M.W., Schneider, W., 2007. The cognitive control network: integrated cortical regions with dissociable functions. Neuroimage 37 (1), 343–360. doi:10.1016/j.neuroimage.2007.03.071.

Corbit, L.H., Muir, J.L., Balleine, B.W., 2003. Lesions of mediodorsal thalamus and anterior thalamic nuclei produce dissociable effects on instrumental conditioning in rats. Eur. J. Neurosci. 18 (5), 1286–1294. doi:10.1046/j.1460-9568.2003.02833.x.

Craig, A.D., 2002. How do you feel? Interoception: the sense of the physiological condition of the body. Nat. Rev. Neurosci. 3 (8), 655–666. doi:10.1038/nrn894.

Davidow, J.Y., Sheridan, M.A., Van Dijk, K.R., Santillana, R.M., Snyder, J., Vidal Bustamante, C.M., …, Somerville, L.H., 2019. Development of prefrontal cortical connectivity and the enduring effect of learned value on cognitive control. J. Cogn. Neurosci. 31 (1), 64–77.

Daw, N.D., O'Doherty, J.P., Dayan, P., Seymour, B., Dolan, R.J, 2006. Cortical substrates for exploratory decisions in humans. Nature 441 (7095), 876–879. doi:10.1038/nature04766.

de Ruiter, M.B., Veltman, D.J., Goudriaan, A.E., Oosterlaan, J., Sjoerds, Z., van den Brink, W., 2009. Response perseveration and ventral prefrontal sensitivity to reward and punishment in male problem gamblers and smokers. Neuropsychopharmacology 34 (4), 1027–1038. doi:10.1038/npp.2008.175.

Deen, B., Pitskel, N.B., Pelphrey, K.A., 2011. In: Three Systems of Insular Functional Connectivity Identified with Cluster Analysis, 21. Cerebral Cortex, New York, N.Y., pp. 1498–1506. doi:10.1093/cercor/bhq186 1991https://doi.org/.

Deng, Y., Wang, X., Wang, Y., Zhou, C., 2018. Neural correlates of interference resolution in the multi-source interference task: a meta-analysis of functional neuroimaging studies. Behav. Brain Funct. 14, 8. doi:10.1186/s12993-018-0140-0.

Eklund, A., Nichols, T.E., Knutsson, H., 2016. Cluster failure: Why fMRI inferences for spatial extent have inflated false-positive rates. PNAS 113 (28), 7900–7905.

Elliott, R., Newman, J.L., Longe, O.A., Deakin, J.F.W., 2003. Differential response patterns in the striatum and orbitofrontal cortex to financial reward in humans: a parametric functional magnetic resonance imaging study. J. Neurosci. 23 (1), 303–307. doi:10.1523/JNEUROSCI.23-01-00303.2003.

Fan, Q., Witzel, T., Nummenmaa, A., Van Dijk, K.R.A., Van Horn, J.D., Drews, M.K., …, Rosen, B.R., 2016. MGH-USC human connectome project datasets with ultra-high b-value diffusion MRI. Neuroimage 124 (0 0), 1108–1114. doi:10.1016/j.neuroimage.2015.08.075.

Fellows, L.K., Farah, M.J., 2003. Ventromedial frontal cortex mediates affective shifting in humans: Evidence from a reversal learning paradigm. Brain 126 (8), 1830–1837. doi:10.1093/brain/awg180.

Gaidica, M., Hurst, A., Cyr, C., Leventhal, D.K., 2018. Distinct populations of motor thalamic neurons encode action initiation, action selection, and movement vigor. J. Neurosci. 38 (29), 6563–6573. doi:10.1523/JNEUROSCI.0463-18.2018.

Galvan, A., Hare, T.A., Parra, C.E., Penn, J., Voss, H., Glover, G., Casey, B.J., 2006. Earlier development of the accumbens relative to orbitofrontal cortex might underlie risk-taking behavior in adolescents. J. Neurosci. 26 (25), 6885–6892. doi:10.1523/JNEUROSCI.1062-06.2006.

Gläscher, J., Hampton, A.N., O'Doherty, J.P., 2009. Determining a role for ventromedial prefrontal cortex in encoding action-based value signals during reward-related decision making. Cereb. Cortex 19 (2), 483–495. doi:10.1093/cercor/bhn098.

Gorgolewski, K., Burns, C.D., Madison, C., Clark, D., Halchenko, Y.O., Waskom, M.L., Ghosh, S.S., 2011. Nipype: a flexible, lightweight and extensible neuroimaging data processing framework in python. Front. Neuroinformat. 5. doi:10.3389/fninf.2011.00013.

Griswold, M.A., Jakob, P.M., Heidemann, R.M., Nittka, M., Jellus, V., Wang, J., … Haase, A. (2002). Generalized autocalibrating partially parallel acquisitions (GRAPPA). Magnetic Resonance in Medicine, 47(6), 1202–1210. https://doi.org/10.1002/mrm.10171

Hampton, A.N., Bossaerts, P., O'Doherty, J.P., 2006. The role of the ventromedial prefrontal cortex in abstract state-based inference during decision making in humans. J. Neurosci. 26 (32), 8360–8367. doi:10.1523/JNEUROSCI.1010-06.2006.

Hughes, M.E., Johnston, P.J., Fulham, W.R., Budd, T.W., Michie, P.T., 2013. Stop-signal task difficulty and the right inferior frontal gyrus. Behav. Brain Res. 256, 205–213. doi:10.1016/j.bbr.2013.08.026.

Jenkinson, M., Bannister, P., Brady, M., Smith, S., 2002. Improved optimization for the robust and accurate linear registration and motion correction of brain images. Neuroimage 17 (2), 825–841. doi:10.1006/nimg.2002.1132.

Jenkinson, M., Beckmann, C.F., Behrens, T.E.J., Woolrich, M.W., Smith, S.M., 2012. FSL. Neuroimage 62 (2), 782–790. doi:10.1016/j.neuroimage.2011.09.015.

Jenkinson, M., Smith, S., 2001. A global optimisation method for robust affine registration of brain images. Med. Image Anal. 5 (2), 143–156. doi:10.1016/S1361-8415(01)00036-6.

Keil, B., Blau, J.N., Biber, S., Hoecht, P., Tountcheva, V., Setsompop, K., …, Wald, L.L., 2013. A 64-channel 3T array coil for accelerated brain MRI. Magn. Reson. Med. 70 (1), 248–258. doi:10.1002/mrm.24427.

Knutson, B., Westdorp, A., Kaiser, E., Hommer, D., 2000. FMRI visualization of brain activity during a monetary incentive delay task. Neuroimage 12 (1), 20–27. doi:10.1006/nimg.2000.0593.

Krebs, R.M., Boehler, C.N., Woldorff, M.G., 2010. The influence of reward associations on conflict processing in the Stroop task. Cognition 117 (3), 341–347. doi:10.1016/j.cognition.2010.08.018.

Kurth, F., Zilles, K., Fox, P.T., Laird, A.R., Eickhoff, S.B., 2010. A link between the systems: Functional differentiation and integration within the human insula revealed by meta-analysis. Brain Struct. Funct. 214 (5–6), 519–534. doi:10.1007/s00429-010-0255-z.

Lanciego, J.L., Luquin, N., & Obeso, J.A. (2012). Functional neuroanatomy of the basal ganglia. Cold Spring Harbor Perspect. Med., 2(12). https://doi.org/ 10.1101/cshperspect.a009621

Lee, J., Shomstein, S., 2013. The differential effects of reward on space- and object-based attentional allocation. J. Neurosci. 33 (26), 10625–10633. doi:10.1523/JNEUROSCI.5575-12.2013.

Liu, X., Hairston, J., Schrier, M., Fan, J., 2011. Common and distinct networks underlying reward valence and processing stages: a meta-analysis of functional neuroimaging studies. Neurosci. Biobehav. Rev. 35 (5), 1219–1236. doi:10.1016/j.neubiorev.2010.12.012.

Menon, V., Uddin, L.Q., 2010. Saliency, switching, attention and control: a network model of insula function. Brain Struct. Funct. 214 (5–6), 655–667. doi:10.1007/s00429-010-0262-0.

Niendam, T.A., Laird, A.R., Ray, K.L., Dean, Y.M., Glahn, D.C., Carter, C.S., 2012. Meta-analytic evidence for a superordinate cognitive control network subserving diverse executive functions. Cognit. Affect. Behav. Neurosci. 12 (2), 241–268. doi:10.3758/s13415-011-0083-5.

Pessiglione, M., Seymour, B., Flandin, G., Dolan, R.J., Frith, C.D., 2006. Dopamine-dependent prediction errors underpin reward-seeking behaviour in humans. Nature 442 (7106), 1042–1045. doi:10.1038/nature05051.

Pessoa, L., Engelmann, J.B., 2010. Embedding reward signals into perception and cognition. Front. Neurosci. 4. doi:10.3389/fnins.2010.00017.

Potenza, M.N., 2008. The neurobiology of pathological gambling and drug addiction: an overview and new findings. Philosoph. Trans. R. Soc. London B 363 (1507), 3181–3189. doi:10.1098/rstb.2008.0100.

Rademacher, L., Krach, S., Kohls, G., Irmak, A., Gründer, G., Spreckelmeyer, K.N., 2010. Dissociation of neural networks for anticipation and consumption of monetary and social rewards. Neuroimage 49 (4), 3276–3285. doi:10.1016/j.neuroimage.2009.10.089.

Robbins, T.W., Gillan, C.M., Smith, D.G., de Wit, S., Ersche, K.D., 2012. Neurocognitive endophenotypes of impulsivity and compulsivity: towards dimensional psychiatry. Trends Cogn. Sci. 16 (1), 81–91. doi:10.1016/j.tics.2011.11.009.

Schultz, W., Dayan, P., Montague, P.R., 1997. A neural substrate of prediction and reward. Science 275 (5306), 1593–1599. doi:10.1126/science.275.5306.1593.

Seeley, W.W., Menon, V., Schatzberg, A.F., Keller, J., Glover, G.H., Kenna, H., …, Greicius, M.D., 2007. Dissociable intrinsic connectivity networks for salience processing and executive control. J. Neurosci. 27 (9), 2349–2356. doi:10.1523/JNEUROSCI.5587-06.2007.

Sescousse, G., Redouté, J., Dreher, J.-C., 2010. The architecture of reward value coding in the human orbitofrontal cortex. J. Neurosci. 30 (39), 13095–13104. doi:10.1523/JNEUROSCI.3501-10.2010.

Setsompop, K., Kimmlingen, R., Eberlein, E., Witzel, T., Cohen-Adad, J., McNab, J.A., …, Wald, L.L., 2013. Pushing the limits of in vivo diffusion MRI for the Human Connectome Project. Neuroimage 80, 220–233. doi:10.1016/j.neuroimage.2013.05.078.

Siegel, J.S., Power, J.D., Dubis, J.W., Vogel, A.C., Church, J.A., Schlaggar, B.L., Petersen, S.E., 2014. Statistical improvements in functional magnetic resonance imaging analyses produced by censoring high-motion data points. Hum. Brain Mapp. 35 (5), 1981–1996. doi:10.1002/hbm.22307.

Smith, S.M., 2002. Fast robust automated brain extraction. Hum. Brain Mapp. 17 (3), 143–155. doi:10.1002/hbm.10062.

Smith, S.M., Jenkinson, M., Woolrich, M.W., Beckmann, C.F., Behrens, T.E.J., Johansen-Berg, H., …, Matthews, P.M., 2004. Advances in functional and structural MR image analysis and implementation as FSL. Neuroimage 23, S208–S219. doi:10.1016/j.neuroimage.2004.07.051.

Swick, D., Ashley, V., Turken, A.U., 2008. Left inferior frontal gyrus is critical for response inhibition. BMC Neurosci. 9, 102. doi:10.1186/1471-2202-9-102.

Tops, M., Boksem, M.A.S., 2011. A potential role of the inferior frontal gyrus and anterior insula in cognitive control, brain rhythms, and event-related potentials. Front. Psychol. 2. doi:10.3389/fpsyg.2011.00330.

Uddin, L.Q., 2015. Salience processing and insular cortical function and dysfunction. Nat. Rev. Neurosci. 16 (1), 55–61. doi:10.1038/nrn3857.

van der Kouwe, A.J.W., Benner, T., Salat, D.H., Fischl, B., 2008. Brain morphometry with multiecho MPRAGE. Neuroimage 40 (2), 559–569. doi:10.1016/j.neuroimage.2007.12.025.

Verbruggen, F., Logan, G.D., 2008. Response inhibition in the stop-signal paradigm. Trends Cogn. Sci. 12 (11), 418–424. doi:10.1016/j.tics.2008.07.005.

Wager, T.D., Rilling, J.K., Smith, E.E., Sokolik, A., Casey, K.L., Davidson, R.J., …, Cohen, J.D., 2004. Placebo-induced changes in FMRI in the anticipation and experience of pain. Science 303 (5661), 1162–1167. doi:10.1126/science.1093065, (New York, N.Y.)https://doi.org/.

Wang, L., Yu, H., Hu, J., Theeuwes, J., Gong, X., Xiang, Y., …, Zhou, X., 2015. Reward breaks through center-surround inhibition via anterior insula. Hum. Brain Mapp. 36 (12), 5233–5251. doi:10.1002/hbm.23004.

Wessel, J.R., O'Doherty, J.P., Berkebile, M.M., Linderman, D., Aron, A.R, 2014. Stimulus devaluation induced by stopping action. J. Experiment. Psychol. General 143 (6), 2316–2329. doi:10.1037/xge0000022.

Wessel, J.R., Tonnesen, A.L., Aron, A.R., 2015. Stimulus devaluation induced by action stopping is greater for explicit value representations. Front. Psychol. 6. doi:10.3389/fpsyg.2015.01640.

Wickens, J.R., Reynolds, J.N., Hyland, B.I., 2003. Neural mechanisms of reward-related motor learning. Curr. Opin. Neurobiol. 13 (6), 685–690. doi:10.1016/j.conb.2003.10.013.

Winter, W., Sheridan, M., 2014. Previous reward decreases errors of commission on later 'No-Go' trials in children 4 to 12 years of age: Evidence for a context monitoring account. Dev. Sci. 17 (5), 797–807. doi:10.1111/desc.12168.

Wittmann, M., Lovero, K.L., Lane, S.D., Paulus, M.P., 2010. Now or later? Striatum and insula activation to immediate versus delayed rewards. Journal of Neuroscience. Psychol. Econ. 3 (1), 15–26. doi:10.1037/a0017252.

Woolrich, M.W., Behrens, T.E.J., Beckmann, C.F., Jenkinson, M., Smith, S.M., 2004. Multilevel linear modelling for FMRI group analysis using Bayesian inference. Neuroimage 21 (4), 1732–1747. doi:10.1016/j.neuroimage.2003.12.023.

Xu, M., Xu, G., Yang, Y., 2016. Neural systems underlying emotional and non-emotional interference processing: an ALE meta-analysis of functional neuroimaging studies. Front. Behav. Neurosci. 10. doi:10.3389/fnbeh.2016.00220.

Zhang, Y., Brady, M., Smith, S., 2001. Segmentation of brain MR images through a hidden Markov random field model and the expectation-maximization algorithm. IEEE Trans. Med. Imaging 20 (1), 45–57. doi:10.1109/42.906424.

Zhang, Z., Mendelsohn, A., Manson, K.F., Schiller, D., Levy, I., 2016. Dissociating value representation and inhibition of inappropriate affective response during reversal learning in the ventromedial prefrontal cortex. ENeuro 2 (6). doi:10.1523/ENEURO.0072-15.2015.